

New Crater Counts on the Lunar Farside. S. Marchi¹, W. F. Bottke², D. A. Kring³, A. Morbidelli⁴, ¹Universite de Nice Sophia-Antipolis, Observatoire de la Cote d'Azur, Nice, France, marchi@oca.eu, ²Center for Lunar Origin and Evolution, Southwest Research Institute, Boulder, CO, ³Center for Lunar Science and Exploration, Lunar and Planetary Institute, Houston, TX, ⁴Observatoire de la Cote d'Azur, Nice, France

Introduction: In order to achieve a better understanding of the early evolution of the Moon and, in particular, its early cratering history, we performed new crater counts on some of the oldest terrains of the lunar farside. We focus our investigation on Pre-Nectarian terrains within the South-Pole Aitken basin (SPA) as well as other Pre-Nectarian terrains outside SPA basin. In this work, we present the derived crater size frequency distributions (SFDs) for these terrains and also discuss their observed differences and similarities. The selected terrains will be used to derive constraints on early lunar cratering during the so-called Pre-Nectarian epoch, namely during the time interval from the formation of the Moon to the formation of Nectaris basin.

New crater counts on Pre-Nectarian terrains: Crater identification and count have been performed on a digital terrain model (DTM) produced by the Lunar Orbiter Laser Altimeter (LOLA) on board the Lunar Reconnaissance Orbiter (LRO) spacecraft [1]. The resolution of the DTM was 64 px/deg, corresponding to 0.4738 km/px. The advantage of these data is that they do not suffer of observational uncertainties due to variation in illumination condition and/or uneven spatial resolution. During the crater identification processes, we also compared LOLA DTM to comparable resolution shaded relief maps produced by Lunar Orbiter and Clementine [2].

Crater counting has been performed with a semi-automated code according to the following steps: i) the regions of interest have been divided in sub-regions of about 10×10 deg²; ii) within each sub-region, craters have been registered by mouse clicking on 5 points over their rims; iii) the 5 selected points are used to fit a circle, returning the center position and the diameter of the craters; iv) all identified craters are saved on a ASCII file for post processing.

In this work we focused on craters >15km to avoid the misleading contributions of secondary craters (i.e., those produced by fragments ejected by other craters [3,4]) to crater statistics in smaller size bins.

In order to validate our crater identification and diameter estimate, we performed several tests with well-known individual craters and crater size frequency distributions over some large basins. Those tests indicate that the discrepancy on crater diameter estimate is of the order of 1-3% for individual craters. We also found that our crater SFDs are in fairly good agreement

(within the error bars) with those published in [4] for terrains near or inside a number of lunar basins (see Figure 1 for some examples).

Discussion and preliminary conclusions: Here we present crater counts on terrains of the lunar farside identified as Pre-Nectarian by geologic mapping methods (see Plate 6B of [4]). Figure 2 shows the terrain selected within SPA basin, while Figure 3 shows our terrain selection in the northern farside (hereinafter PNT).

The resulting crater SFDs from SPA and PNT are indistinguishable in the crater size range from 50 km to 160 km (see Figure 4). For craters size <50km, SPA has a shallower slope than PNT, therefore SPA is less and less cratered than PNT for decreasing crater sizes. At crater diameter of 15 km, the PNT/SPA ratio is about 1.5. Note that the crater SFD is relatively constant within PNT terrains, thus we tend to exclude contamination by secondary craters due to more recent large basin, like Imbrium. For crater size >160km, the observed differences are due to the number of basins considered in each crater count. For PNT the following basins have been included: Birkhoff, Coulomb-Sarton, Freundlich-Sharonov, Lorentz. For SPA, Apollo, Planck and Poincare basins have been included. Schrödinger basin and its ejecta have been excluded at this stage since they clearly formed after the Nectaris basin. It must be noticed, however, that adding Schrödinger and other basins to SPA would not significantly reduce the difference respect to PNT.

The nature of the observed differences and similarities is not clear yet. Several scenarios may be compatible with the observed crater SFDs.

For instance, the overlapping of SPA and PNT at intermediate crater range, may be an indication of similar age for these terrains. Therefore, the observed differences might be due to local phenomena (such as differences in the terrain properties which, for instance, alter the crater scaling law; or subsequent episodes of crater obliteration).

On the other hand, the differences in the crater SFDs of SPA and PNT might be due to variations in the impactor size distribution. Several dynamical scenarios may account for a variation in the impactor flux able to explain the trends for crater sizes <50km. Nevertheless, such a variation must have taken place in a very short time interval given the overlap of SPA and PNT at the intermediate size range.

While the results presented here are still preliminary, they appear to provide new insights into the most ancient times still recorded on the Moon. The next task is to refine the analysis by studying other terrains as well as modeling the evolution of the population that created these craters following the approach done by [6].

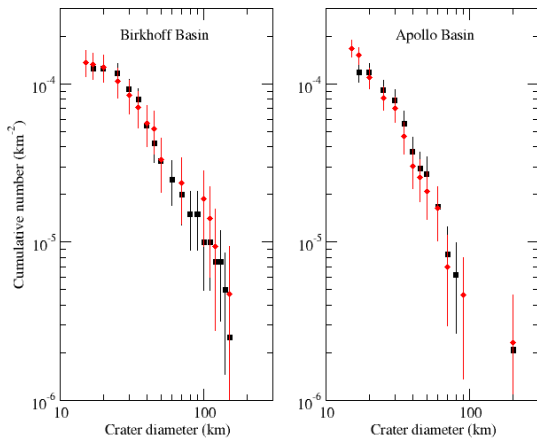


Figure 1: Comparison of our own crater size frequency distributions (red diamonds) of Apollo and Birkhoff basins with published data from [4] (black squares). The residual differences is likely due to a different choice of the terrains used.

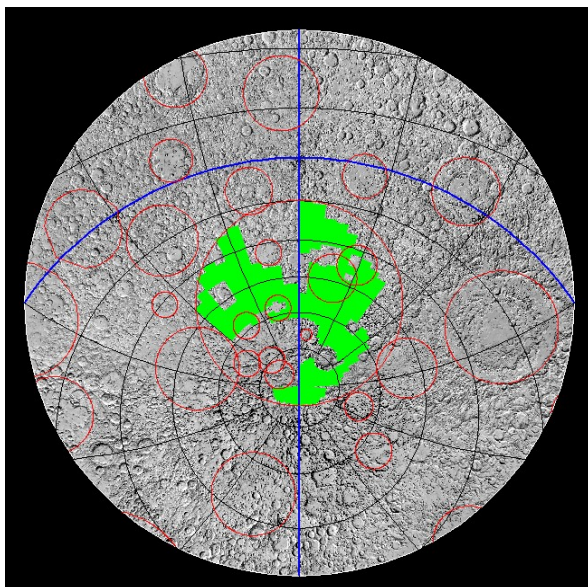


Figure 2: Pre-Nectarian terrains selected within SPA basin. Red circles indicate the major lunar basins.

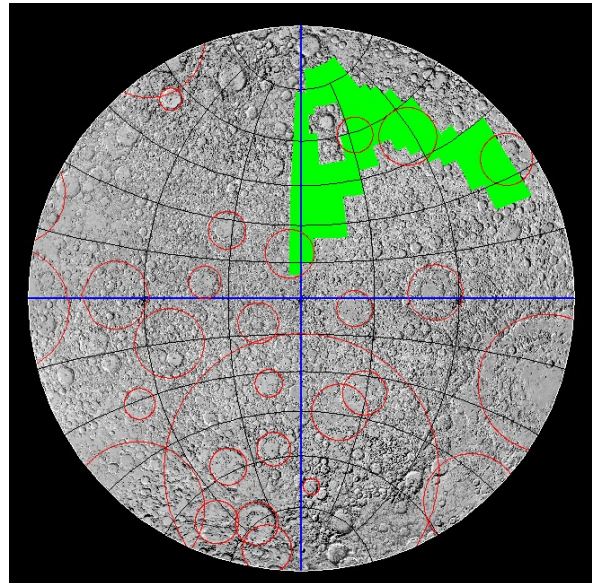


Figure 3: Pre-Nectarian terrains selected in the northern farside. Red circles indicate the major lunar basins.

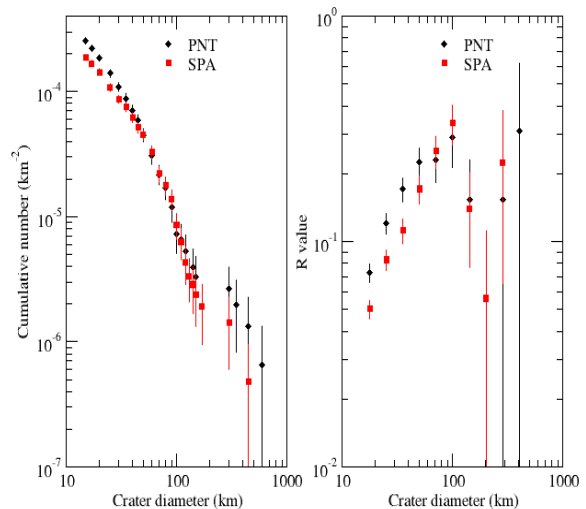


Figure 4: Crater size frequency distributions for PNT and SPA. Left panel: Cumulative data; Right panel: R-values.

References: [1] Smith D. E. et al. (2010) *Geoph. Jour. Res.* 37, 18204 [2] Data available here: <http://www.mapaplanet.org/explorer/moon.html> [3] Wilhelms et al. (1978) *Proc. Lunar Planet. Sci. Conf 9th p. 3735-3762.* [4] Wilhelms (1987) *U.S. Geol. Surv. Prof. Pap. 1348, 302 pp.* [5] Neukum and Ivanov Hazards due to Comets and Asteroids, (1994) 359. [6] Marchi et al. (2009) *AJ* 137, 4936.